

# CLUSTER PARAMETERS FOR TIME-VARIANT MIMO CHANNEL MODELS

N. Czink<sup>1,2</sup>, R. Tian<sup>3</sup>, S. Wyne<sup>3</sup>, G. Eriksson<sup>3,4</sup>, T. Zemen<sup>2</sup>, J. Ylitalo<sup>5</sup>, F. Tufvesson<sup>3</sup>, and A. F. Molisch<sup>3,6</sup>

<sup>1</sup>*Institut für Nachrichtentechnik und Hochfrequenztechnik, Technische Universität Wien, Vienna, Austria*

<sup>2</sup>*Forschungszentrum Telekommunikation Wien (ftw.), Vienna, Austria*

<sup>3</sup>*Department of Electrical and Information Technology, Lund University, Sweden*

<sup>4</sup>*FOI Swedish Defence Research Agency, Linköping, Sweden*

<sup>5</sup>*Elektrobit Corp., Finland*

<sup>6</sup>*Mitsubishi Electric Research Labs, Cambridge, MA, USA*

## ABSTRACT

The next challenge for MIMO radio channel models is to simulate the time-variant nature of the channel correctly. Cluster-based MIMO channel models are well suited for this problem, however they currently lack an accurate parameterization of the time-variant cluster parameters.

In this paper we identify and track clusters from three different measurements conducted in an indoor, a sub-urban, and a rural environment. The time-variant cluster parameters of interest are: (i) cluster movement, (ii) change of cluster spreads, (iii) cluster lifetimes, and birth and death rates of cluster.

We find that clusters show significant movement in parameter space depending on the environment. The spreads of individual clusters change rather randomly over their lifetime, with a standard deviation up to 150% of their mean spread. The cluster lifetime is approximately exponentially distributed, however additionally one has to account for long-living clusters coming from the line-of-sight path or from major reflectors.

Key words: cluster-based channel modelling; MIMO; double-directional radio channel.

## 1. INTRODUCTION

In MIMO channels, multipath components (MPCs) occur in clusters, i.e. groups of MPCs that are co-located in delay, direction of arrival (DoA), and direction of departure (DoD) [1–3]. Taking the clustered nature of the MPCs into account is very important for system design. For example, disregarding it leads to an overestimation of channel capacity [4, 5]. Furthermore, clusters can be efficiently described by their mean position in the parameter space, and by their spreads. By this concept, the radio channel is modelled in a physical way while using only few parameters.

For this reason, many state-of-the-art MIMO channel models rely on the concept of multipath clusters [6]. In particular, the majority of standardized MIMO channel models, like 3GPP-SCM [7], IEEE 802.11n [8], COST 259 DCM [9, 10], and COST 273 [11] are cluster based.

Time variations of the channels occur, e.g. when the mobile station moves along a route. In a clustered model,

they can be modelled by cluster movement, where cluster parameters evolve smoothly over time, and by the cluster birth and death rate.

In order to consistently parameterize such clustered time-variant MIMO models, clusters need to be jointly identified and tracked in time-variant MIMO channel measurements. In [12], we proposed a comprehensive solution to jointly identify and track clusters in the delay/DoA/DoD-domain.

In this paper we use this joint clustering-and-tracking framework on three different kinds of MIMO channel measurements: (i) indoor measurements at 2.55 GHz, (ii) outdoor suburban measurements at 2.0 GHz, (iii) outdoor rural measurements at 300 MHz. The cluster parameters of interest include cluster movement (change of cluster position in parameter space), the change of cluster spreads, the lifetime of clusters and the cluster birth and death rates.

This paper is organised as follows. Section 2 provides a brief overview of the data processing. In Section 3 we detail the different measurements used. The results are presented in Section 4. Section 5 concludes this paper.

## 2. METHOD

For our evaluations we use the automatic clustering-and-tracking algorithm presented in [12]. This algorithm combines the KPowerMeans clustering algorithm [13] used to identify clusters from measurements with a Kalman filter for tracking the clusters between different snapshots of the measurements.

Starting point for the algorithm is a time-variant channel measurement. The recorded snapshots of the impulse responses are post-processed to estimate propagation paths. Snapshots are measurements of the MIMO channel at specific time instants.

The input data for the clustering-and-tracking algorithm are a number of propagation paths for each snapshot of the recorded channel. The snapshots of the measured MIMO impulse responses are post-processed by a high-resolution estimation algorithm to identify the parameters of the propagation paths. To make the tracking more robust, we use a sliding window over two snapshots, and set

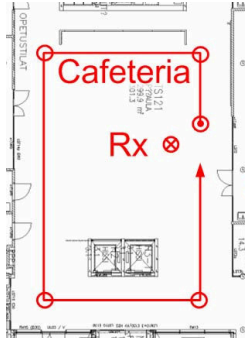


Figure 1. Floorplan of the indoor scenario

the cluster power threshold to 2.5% (in contrast to using 1% as indicated in [12, Sec. III.B]).

The outcome of the algorithm is a number of tracked clusters and, for every tracked cluster its parameters for the snapshots it exists in. These parameters are the cluster position (delay, DoA, DoD), the cluster spreads (delay spread, DoA spread, DoD spread), the cluster power, and its lifetime. Based on these parameters, we evaluate the time-variant behaviour of the clusters.

### 3. MEASUREMENTS

In this paper we compare data from three different channel sounding campaigns conducted by different institutions.

#### 3.1. Campaign I — indoor scenario

These measurements were conducted at the University of Oulu, Finland using an Elektorbit Propsound CS<sup>TM</sup> wideband radio channel sounder at a center frequency of 2.55 GHz [14]. Snapshots of the radio channel were recorded approximately every  $0.45\lambda$ . The recorded impulse responses were post-processed using the ISIS (initialization-and-search improved SAGE) algorithm to estimate single propagation paths [15].

In this paper we discuss results from a line-of-sight (LOS) measurement route in a cafeteria (see Figure 1). The Rx was placed on a table, while the Tx was moved along the indicated route in the room over a distance of 44 m corresponding to  $295\lambda$ . Because of many metal chairs and tables, and the quite reflective walls, we expected rich scattering in the channel apart from the LOS component. However, it turned out that the observed channels were still pretty directive.

#### 3.2. Campaign II — outdoor sub-urban environment

The data were collected in a small town called Weikendorf, northwest of Vienna, Austria. For the measurements we used a RUSK MEDAV channel sounder operating at a center frequency of 2.0 GHz [16]. Snapshots of the radio channel were recorded approximately every  $1.6\lambda$ . The recorded impulse responses were also post-processed using the ISIS algorithm to estimate the propagation paths.

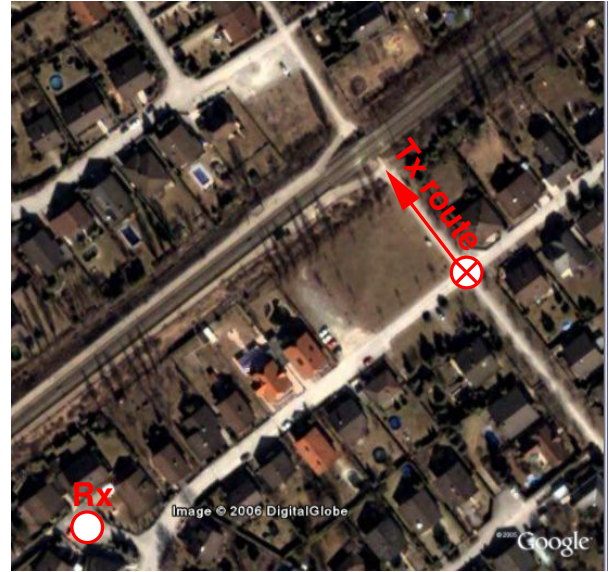


Figure 2. Sub-urban environment

The measurement route (see Figure 2) was along a road towards a railway tunnel, mostly with LOS, partly with obstructed LOS. The total distance traveled was 53 m corresponding to  $353\lambda$ . The channel is quite directive at the Rx side, but shows rich scattering around the Tx.

#### 3.3. Campaign III — outdoor rural environment

The third set of measurements were conducted in an outdoor scenario in the 300 MHz band using the RUSK Lund MIMO channel sounder. A description of the measurement campaign can be found in [17].

The measurement route used in this paper (see Figure 3) is approximately 320 m long, corresponding to  $320\lambda$ . The snapshot spacing used in this paper is approximately  $0.97\lambda$ . The measured impulse responses were post-processed by a SAGE algorithm [15] to obtain propagation paths for each snapshot of the channel.

## 4. RESULTS

This paper focuses on the *time-variance* of the cluster parameters, i.e. how much do the cluster parameters change during the existence of the individual clusters.

We focus on (i) the change of the cluster position over the travelled wavelength (“cluster movement”), (ii) the change of the cluster spreads, (iii) the cluster lifetime and cluster birth and death rates.

#### 4.1. Cluster movement

Figure 4 exemplifies the cluster mean delay for one individually selected cluster from each environment. The cluster mean delay varies significantly in the presented indoor environment (Figure 4a), it seems that the cluster jitters around a steady increase. Also in the sub-urban environment (see Figure 4b), the cluster is changing its position quite strongly over its lifetime. This cluster is likely to combine two scatterers. The steep decrease in delay is likely to come from a change in the propagation

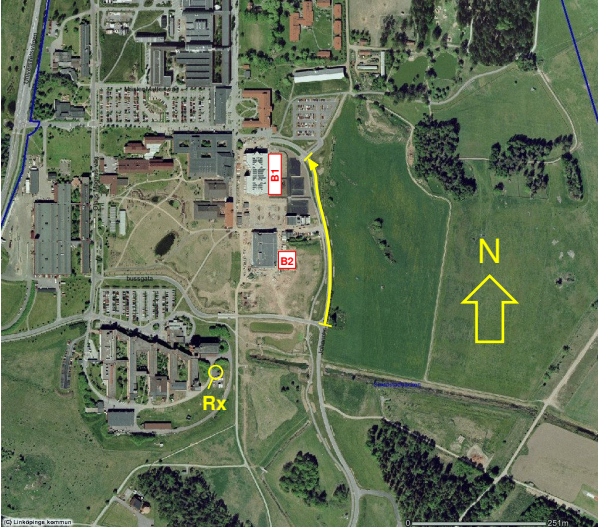


Figure 3. Rural environment

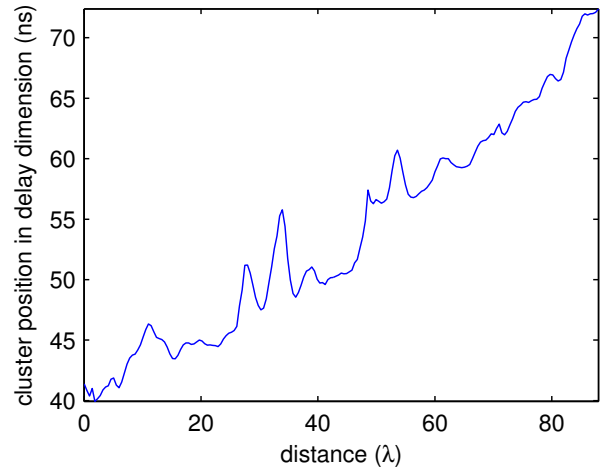
conditions, where the scatterer with shorter delay grew stronger, thus making the cluster delay smaller. In the rural environment (Figure 4c), the strong movement during the first few snapshots seems to be an artifact of the tracking algorithm. The Kalman tracking needs some training to keep track of the cluster. After these first snapshots, the cluster delay increases almost steadily.

We describe the cluster movement by the change of the cluster mean parameters related to travelling one wavelength with the transmitter. In the following we will present the average cluster movement of all clusters identified in the three environments. Since the sample mean of the parameters is strongly influenced by the artifacts, we decided to use the *median* of the sample instead. Figures 5–7 show histograms of these movement parameters. The mean cluster delay changes within the range of  $-5 \dots 5$  ns per wavelength (see Figure 5). Strong changes can again be attributed to the combination of more than one propagation effect in one cluster.

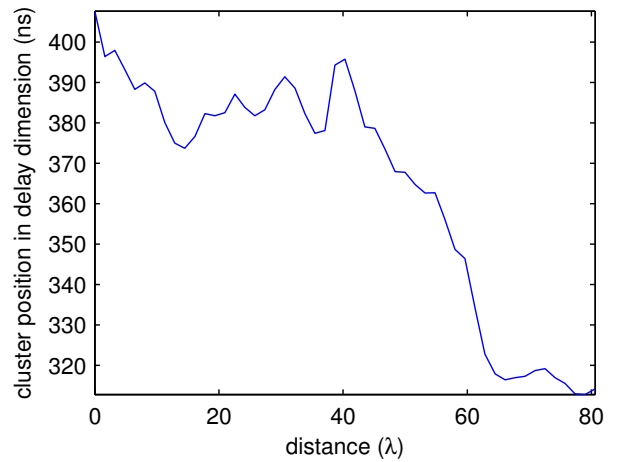
The median cluster changes in AoA (see Figure 6) are particularly interesting, since we observe significant differences in the histograms for the different environments. This effect can be attributed to the very different propagation environments. In the indoor scenario, there was strong scattering around both the Rx and Tx, leading also to stronger cluster movement around the Rx. In the sub-urban scenario, the observed values are quite small. The Rx did not experience local scattering since it was placed on a crane overlooking the environment. In the rural environment, there was also strong scattering around the Rx, where the movement of the Tx led to cluster movement on the Rx side. The mean cluster changes in AoD shown in Figure 7 are quite similar for all environments.

#### 4.2. Change of cluster spreads

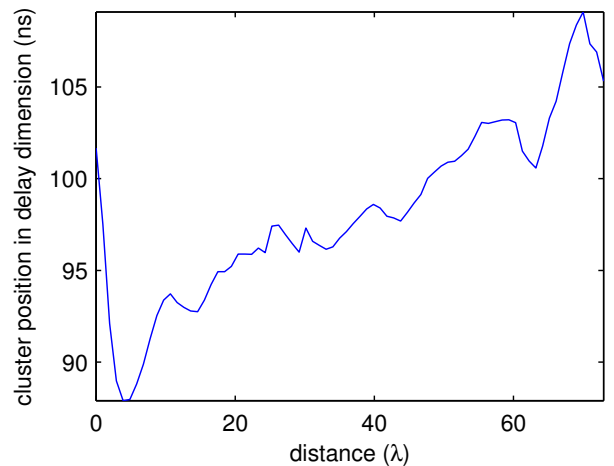
Another figure of merit is how much the cluster spreads change during the lifetime of one cluster. Figure 8 shows the cluster delay spread of one individually selected cluster for the environments. In all three environments we



(a) indoor

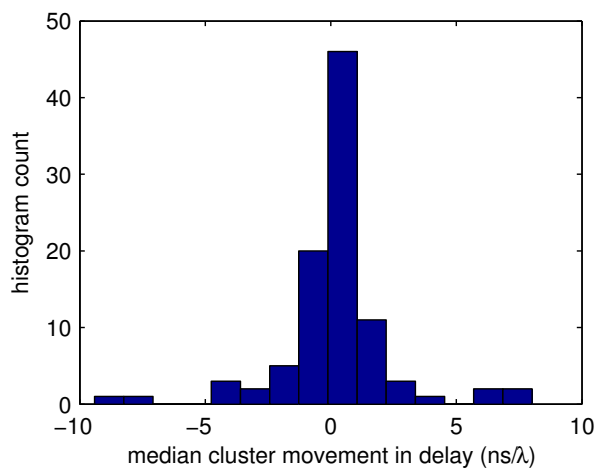


(b) sub-urban

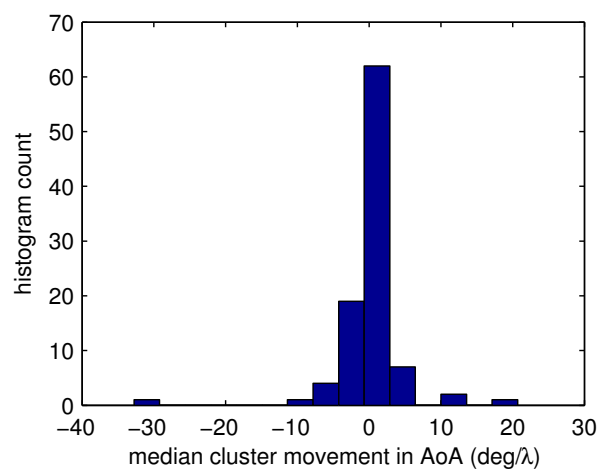


(c) rural

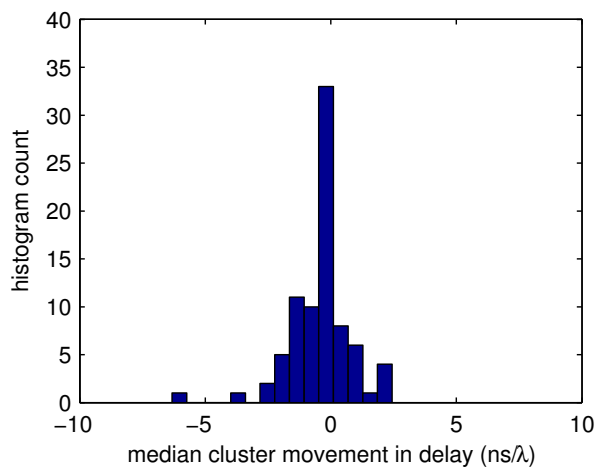
Figure 4. Cluster movement in delay dimension



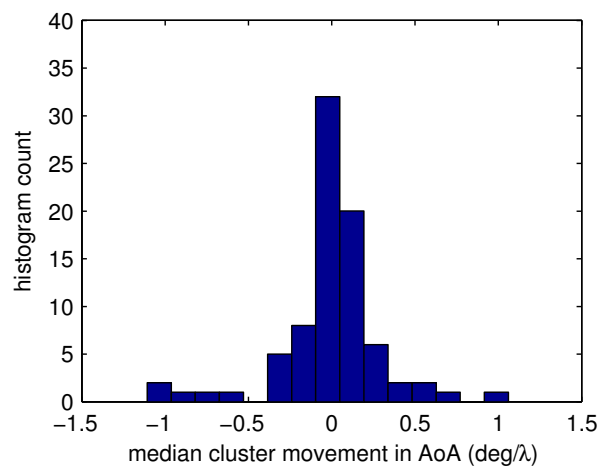
(a) indoor



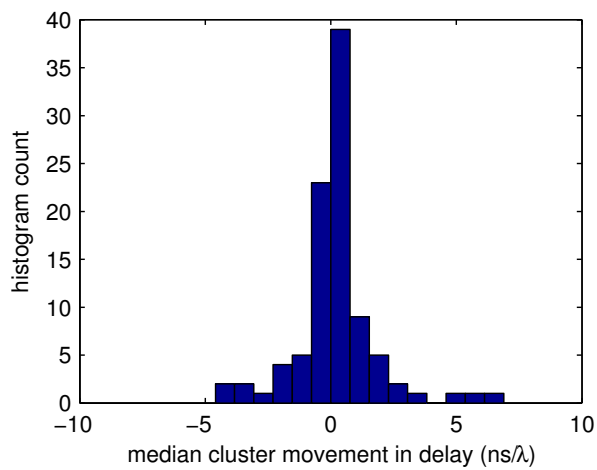
(a) indoor



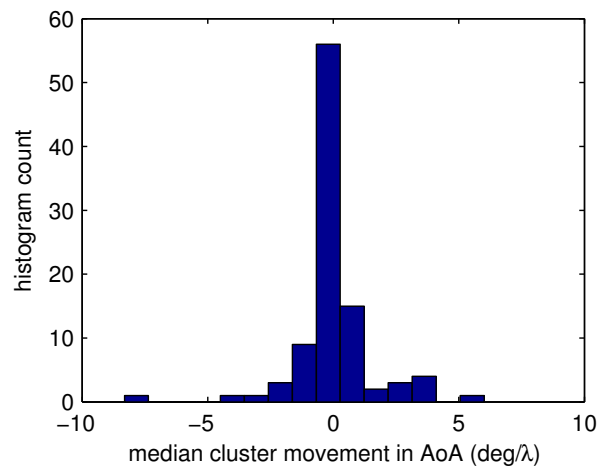
(b) sub-urban



(b) sub-urban



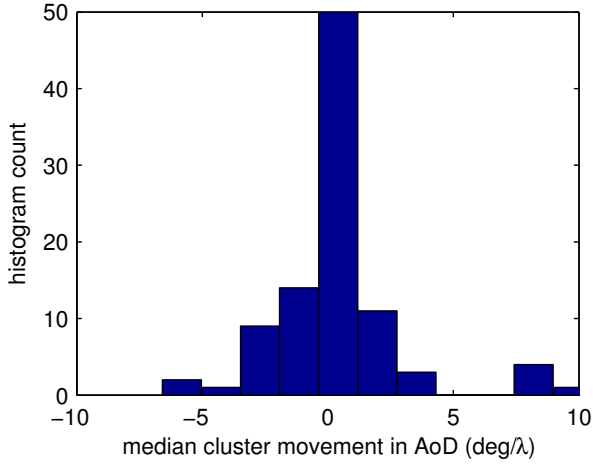
(c) rural



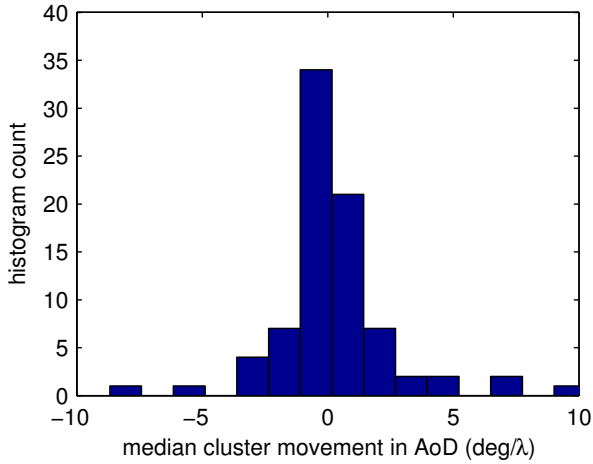
(c) rural

Figure 5. Median cluster movement in delay

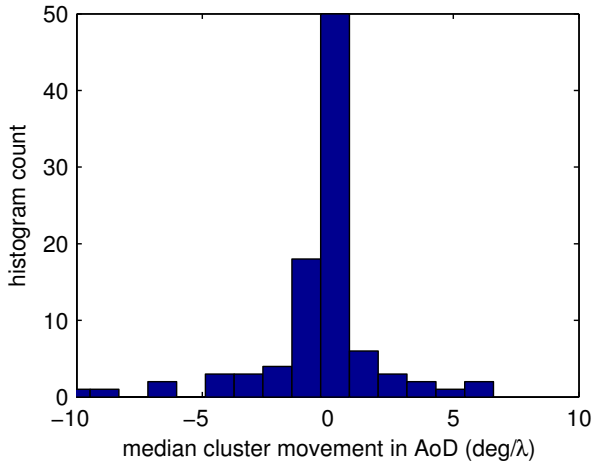
Figure 6. Median cluster movement in AoA



(a) indoor



(b) sub-urban



(c) rural

Figure 7. Median cluster movement in AoD

observe that the delay spread changes significantly over the traveled distance. These changes seem to be rather random. Moreover, we also observe some kind of outliers, which may again be an artifact of the clustering-and-tracking algorithm.

In order to quantify these changes, we use a deviation measure similar to the standard deviation of the cluster spread with following changes: (i) we use the median instead of the mean in order to mitigate the effect of outliers, (ii) we relate the deviation to the median value of the cluster spread to obtain a spread in percent. We calculate this spread deviation as

$$\mathcal{D}_\tau = \frac{\sqrt{\frac{1}{N} \sum_{k=1}^N (\sigma_{\tau,k} - \bar{\sigma}_\tau)^2}}{\bar{\sigma}_\tau},$$

where  $\sigma_{\tau,k}$  denotes the cluster delay spread at snapshot  $k$ ,  $\bar{\sigma}_\tau$  denotes the cluster *median* delay spread over all snapshots, and  $N$  is the lifetime of the regarded cluster. The deviations for the AoA and AoD cluster spreads are defined similarly.

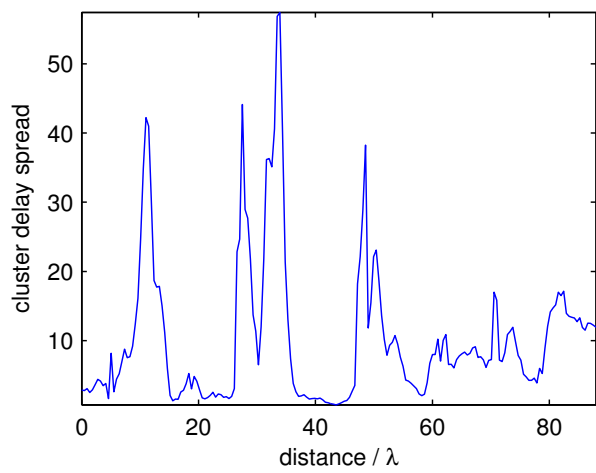
Figure 9 shows the the histograms of the deviation for all three cluster dimensions. We first observe a similar behaviour for all three dimensions AoA, AoD and delay. a standard deviation around 50% of the cluster spread value is most probable. Surprisingly, the results are quite similar in all different environments. Values above 100% indicate that some clusters tend to grow for short periods, where they show considerably larger spreads than the median spread. In these cases, the clustering algorithm (accidentally, or for a good reason) combines wider-spread paths into one cluster. This effect occurs when some weak outlying propagation paths exist for just a few snapshots and then vanish again. Such paths are allocated to the closest cluster.

### 4.3. Cluster lifetimes, birth and death rates

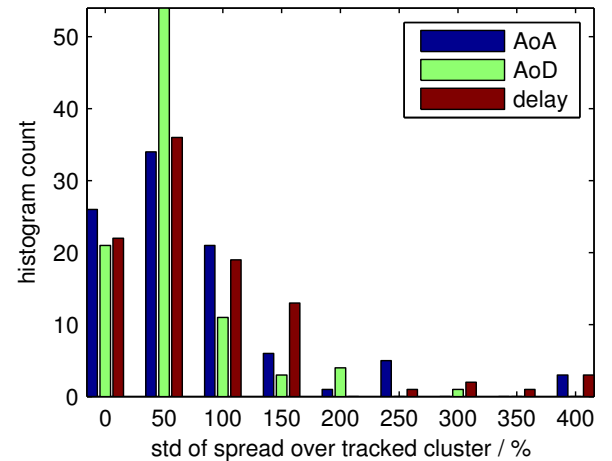
Important parameters for cluster-based models are the lifetime of clusters and how strongly the number of clusters changes between different snapshots.

Figure 10 shows histograms of the cluster lifetimes for the different environments. Like in [16], the plots give rise to the assumption of an exponential distribution of the lifetime. However, we also observe a number of clusters with significantly larger lifetime. We particularly evaluated this effect for the rural environment and found that these long-living clusters come from the LOS path and from dominant reflectors in the channel. Thus, these clusters do have significant impact and must not be neglected when modelling the radio channel.

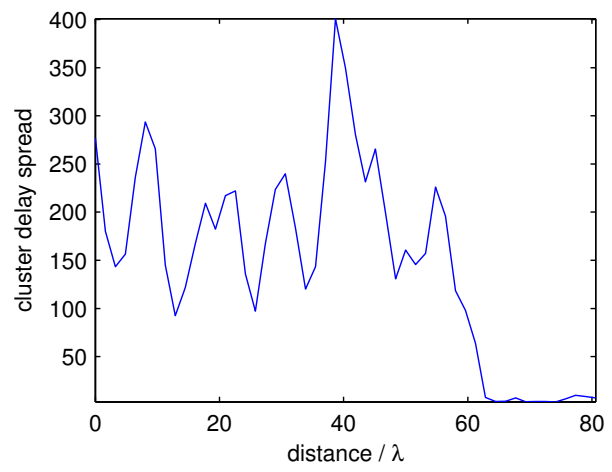
The birth rates and death rates of the clusters are evaluated in Figure 11. The histograms show the number of newly born or died clusters evaluated for all snapshots. It is evident that a change of one or two clusters in a snapshot is quite probable. Only in very few cases, three or more clusters are born or die at the same snapshot. Again, the results are fairly similar for all environments which leads to the conclusion that clusters can be tracked quite well.



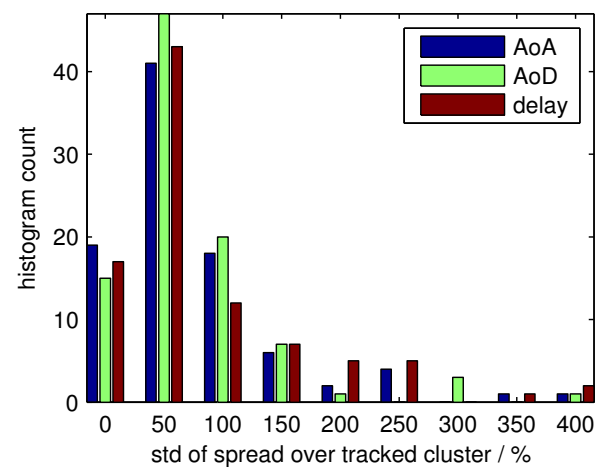
(a) indoor



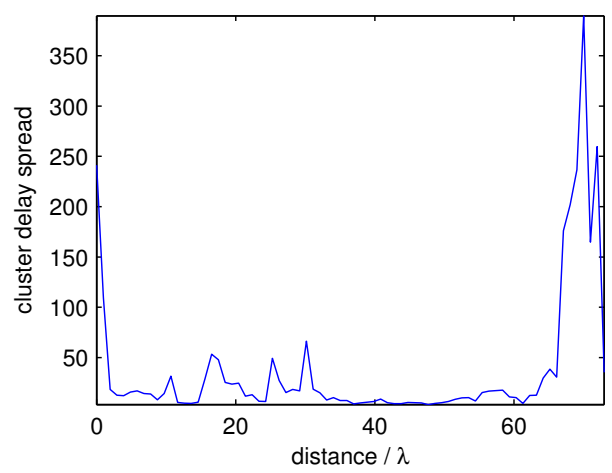
(a) indoor



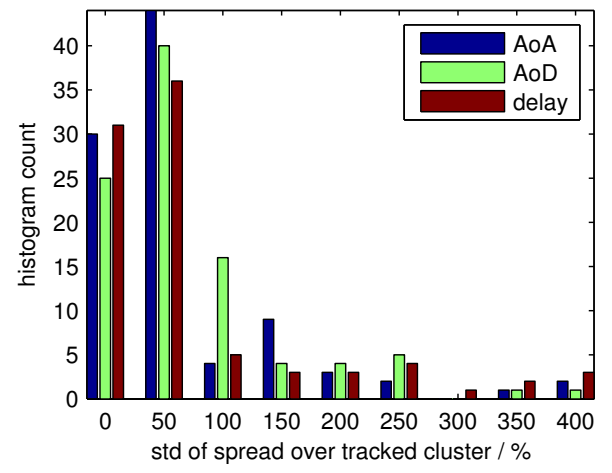
(b) sub-urban



(b) sub-urban



(c) rural



(c) rural

Figure 8. Change of the cluster delay spread

Figure 9. Standard deviations of the change of the cluster delay spreads in percent of the median delay spread

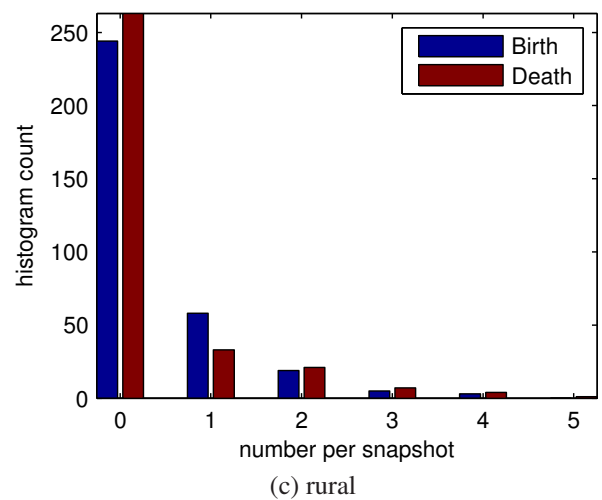
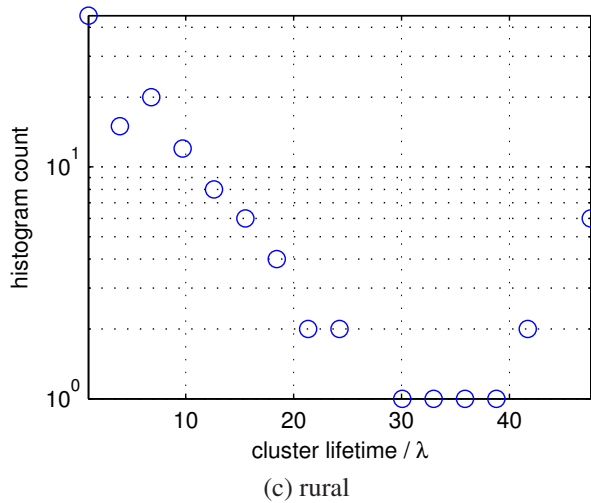
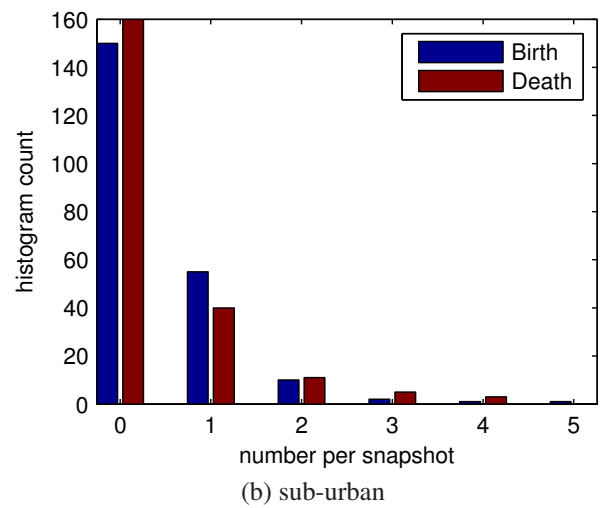
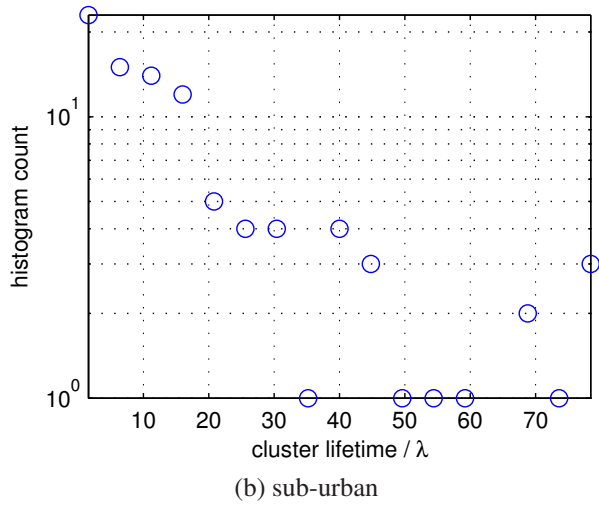
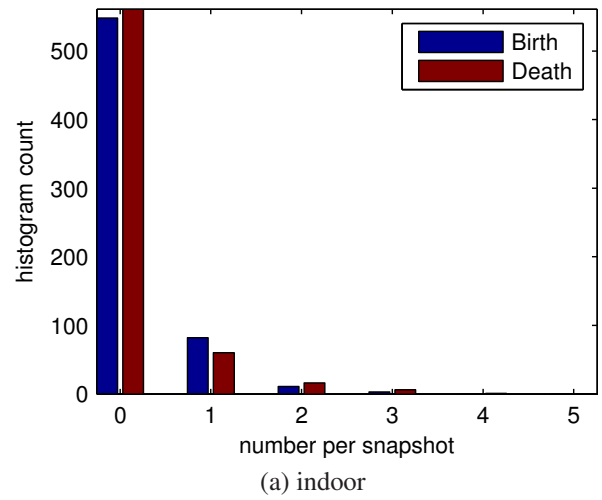
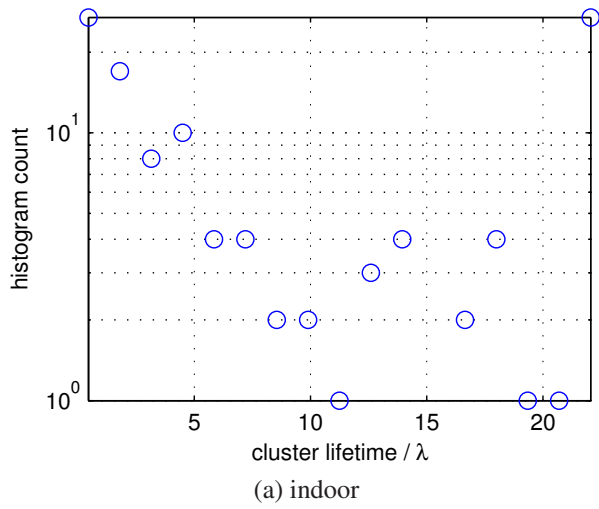


Figure 10. Cluster lifetimes in terms of wavelengths

Figure 11. Cluster birth and death rate per snapshot

## 5. CONCLUSIONS

In this paper we evaluated the time-variant behaviour of multipath clusters from MIMO channel measurements in three different environments.

Our results show that clusters move significantly in the parameter domain. Some of these movements are quite strong, which can be attributed to changing propagation conditions in these particular clusters.

The cluster spreads are also strongly varying over the lifetime of the individual clusters with a deviation of up to 150% around their median value. This effect is due to the allocation of short-living outlying paths to dominant clusters.

Cluster lifetimes are approximately exponentially distributed. However, the line-of-sight cluster, and clusters from dominant reflections need to be accounted for individually, since they show a much longer lifetime.

Our results show that the environment plays a significant role for the cluster movement parameters and for the cluster lifetimes, while the mean deviation of the spreads is quite similar in all environments.

## ACKNOWLEDGEMENTS

This work was initiated by a short-term scientific mission in the framework of the EC project COST 2100. We thank Elektrobit Corp. for generous support. Research reported here was also supported by the Kplus program, an INGVAR grant from the Swedish SSF, and the SSF-Center of Excellence for High-Speed Wireless Communications. We acknowledge the Swedish Defense Research Agency (FOI) for providing the 300 MHz measurement data.

## REFERENCES

1. Q. H. Spencer, B. D. Jeffs, M. A. Jensen, and A. L. Swindlehurst, "Modeling the statistical time and angle of arrival characteristics of an indoor multipath channel," *IEEE Journal on Selected Areas in Communications*, vol. 18, pp. 347 – 359, March 2000.
2. C.-C. Chong, C.-M. Tan, D. Laurenson, S. McLaughlin, M. Beach, and A. Nix, "A new statistical wide-band spatio-temporal channel model for 5-GHz band WLAN systems," *IEEE Journal on Selected Areas in Communications*, vol. 21, no. 2, pp. 139 – 150, Feb. 2003.
3. M. Toeltsch, J. Laurila, A. F. Molisch, K. Kalliola, P. Vainikainen, and E. Bonek, "Spatial characterization of urban mobile radio channels," *IEEE JSAC*, vol. 20, pp. 539–549, 2002.
4. K. Li, M. Ingram, and A. Van Nguyen, "Impact of clustering in statistical indoor propagation models on link capacity," *IEEE Transactions on Communications*, vol. 50, no. 4, pp. 521 – 523, April 2002.
5. A. F. Molisch, "Effect of far scatterer clusters in MIMO outdoor channel models," in *Proc. 57th IEEE Vehicular Techn. Conf.*, 2003, pp. 534–538.
6. P. Almers, E. Bonek, A. Burr, N. Czink, M. Debbah, V. Degli-Esposti, H. Hofstetter, P. Kyösti, D. Laurenson, G. Matz, A. Molisch, C. Oestges, and H. Özcelik, "Survey of channel and radio propagation models for wireless MIMO systems," *EURASIP Journal on Wireless Communications and Networking*, 2007.
7. "Spatial channel model for Multiple Input Multiple Output (MIMO) simulations (3GPP TR 25.996), v6.1.0," Sep. 2003. [Online]. Available: [www.3gpp.org](http://www.3gpp.org)
8. V. Erceg *et al.*, "TGn Channel Models," IEEE P802.11 Wireless LANs, Tech. Rep., May 2004, <http://www.802wirelessworld.com:8802/>.
9. A. F. Molisch, H. Asplund, R. Heddergott, M. Steinbauer, and T. Zwick, "The COST 259 directional channel model – I. overview and methodology," *IEEE Transactions on Wireless Communications*, vol. 5, pp. 3421–3433, 2006.
10. H. Asplund, A. A. Glazunov, A. F. Molisch, K. I. Pedersen, and M. Steinbauer, "The COST 259 directional channel model – II. macrocells," *IEEE Transactions on Wireless Communications*, vol. 5, pp. 3434–3450, 2006.
11. L. Correia, Ed., *Mobile Broadband Multimedia Networks*. Academic Press, 2006.
12. N. Czink, R. Tian, S. Wyne, F. Tufvesson, J.-P. Nuutinen, J. Ylitalo, E. Bonek, and A. F. Molisch, "Tracking time-variant cluster parameters in MIMO channel measurements," in *ChinaCom 2007*, Shanghai, China, August 2007.
13. N. Czink, P. Cera, J. Salo, E. Bonek, J.-P. Nuutinen, and J. Ylitalo, "A framework for automatic clustering of parametric MIMO channel data including path powers," in *IEEE Vehicular Technology Conference 2006 Fall*, Montreal, Canada, 2006.
14. N. Czink, E. Bonek, L. Hentilä, J.-P. Nuutinen, and J. Ylitalo, "Cluster-based MIMO channel model parameters extracted from indoor time-variant measurements," in *IEEE GlobeCom 2006*, San Francisco, USA, Nov. 2006.
15. B. Fleury, P. Jourdan, and A. Stucki, "High-resolution channel parameter estimation for MIMO applications using the SAGE algorithm," in *2002 International Zurich Seminar on Broadband Communications*, Zurich, Feb. 2002, pp. 30–1 – 30–9.
16. N. Czink, G. D. Galdo, and C. F. Mecklenbräuker, "A novel cluster tracking algorithm," in *IEEE Personal Indoor and Mobile Radio Communications (PIMRC) 2006*, September 2006.
17. G. Eriksson, F. Tufvesson, and A. F. Molisch, "Propagation channel characteristics for peer-to-peer multiple antenna systems at 300 MHz," in *IEEE GlobeCom 2006*, San Francisco, USA, Nov. 2006.